



Calhoun: The NPS Institutional Archive
DSpace Repository

Faculty and Researchers

Faculty and Researchers' Publications

2010-06

A conserved minimal adjustment scheme for stabilization of hydrographic profiles

Fan, Chenwu; Chu, Peter C.

Chu, P.C., and C.W. Fan, 2010: A conserved minimal adjustment scheme for stabilization of hydrographic profiles. *Journal of Atmospheric and Oceanic Technology*, American Meteorological Society, Vol. 27 (6), 1072-1083 (paper download).
<https://hdl.handle.net/10945/36095>

This publication is a work of the U.S. Government as defined in Title 17, United States Code, Section 101. Copyright protection is not available for this work in the United States.

Downloaded from NPS Archive: Calhoun



Calhoun is the Naval Postgraduate School's public access digital repository for research materials and institutional publications created by the NPS community. Calhoun is named for Professor of Mathematics Guy K. Calhoun, NPS's first appointed -- and published -- scholarly author.

Dudley Knox Library / Naval Postgraduate School
411 Dyer Road / 1 University Circle
Monterey, California USA 93943

<http://www.nps.edu/library>

A Conserved Minimal Adjustment Scheme for Stabilization of Hydrographic Profiles

PETER C. CHU AND CHENWU FAN

Department of Oceanography, Naval Postgraduate School, Monterey, California

(Manuscript received 25 September 2009, in final form 26 January 2010)

ABSTRACT

Ocean (T, S) data analysis/assimilation, conducted in the three-dimensional physical space, is a generalized average of purely observed data (data analysis) or of modeled/observed data (data assimilation). Because of the high nonlinearity of the equation of the state of the seawater and nonuniform vertical distribution of the observational profile data, false static instability may be generated. A new analytical conserved adjustment scheme has been developed on the base of conservation of heat, salt, and static stability for the whole water column with predetermined (T, S) adjustment ratios. A set of well-posed combined linear and nonlinear algebraic equations has been established and is solved using Newton's method. This new scheme can be used for ocean hydrographic data analysis and data assimilation.

1. Introduction

Raw and averaged observational hydrographic data contain substantial regions with vertical density inversions. For example, Jackett and McDougall (1995) found that the annually averaged field of the ocean atlas of Levitus (1982) had more than 44% of the casts possessing static instability at least at one level. Here, the word "cast" is used to denote a pair of vertical temperature and salinity profiles. A widely used concept for static stability E is defined by Lynn and Reid (1968) as "the individual density gradient by vertical displacement of a water parcel (as opposed to the geometric density gradient)." For discrete samples (T_k, S_k) at depth $z_k, k = 1, 2, \dots, K$ (k increasing downward), the density difference between two adjacent levels is taken after one is adiabatically displaced to the depth of the other. Computationally, E_k is calculated by

$$E_k = \rho(S_{k+1}, T_{k+1}, z_k) - \rho(S_k, T_k, z_k), \quad (1)$$

$$k = 1, 2, \dots, K - 1,$$

where $\rho(S_{k+1}, T_{k+1}, z_k)$ is the local potential density of the lower of the two adjacent levels between z_k and z_{k+1} , with respect to the upper of the two adjacent levels z_k ,

and ρ is the in situ density to the depth of the upper of the two adjacent levels z_k . The density inversion is defined by the occurrence of the negative value of E_k . The minimum static stability is represented by $E_k = E_{\min}$. It is not always possible to reach zero exactly due to the precision limitations of the temperature and salinity values used (Locarnini et al. 2006). As a result, the minimum value for the static stability is given by

$$E_k \geq E_{\min}, \quad k = 1, 2, \dots, K, \quad (2)$$

where E_{\min} is the reference value for the minimum static stability, which is user-defined. If static instability occurs in an observed or averaged hydrographic cast [i.e., (2) is not satisfied], this profile needs to be adjusted.

The National Oceanographic Data Center (NODC) uses a local interactive (T, S) separated adjustment method (Locarnini et al. 2006), which is based on the method proposed by Jackett and McDougall (1995) with some modifications, to minimally adjust unstable temperature and salinity profiles (hereafter referred to as the MA method)

$$\mathbf{x} = (T_1, T_2, \dots, T_K, S_1, S_2, \dots, S_K)$$

into stable profiles

$$\mathbf{x} + \Delta\mathbf{x} = (T_1 + \Delta T_1, T_2 + \Delta T_2, \dots, T_K + \Delta T_K, S_1 + \Delta S_1, S_2 + \Delta S_2, \dots, S_K + \Delta S_K).$$

Corresponding author address: Dr. Peter C. Chu, Naval Ocean Analysis and Prediction (NOAP) Lab, Naval Postgraduate School, 833 Dyer Rd., Monterey, CA 93940.
E-mail: pcchu@nps.edu

After assuming T and S are linear, the adjustment is to solve the problem:

$$\text{Minimize } \|\Delta \mathbf{x}\| \quad \text{subject to} \quad \mathbf{A} \cdot (\mathbf{x} + \Delta \mathbf{x}) \geq E_{\min}, \quad (3)$$

where the finite-difference approximation of stability E_k becomes the inner product of the matrix \mathbf{A} and the profile vector $\mathbf{x} + \Delta \mathbf{x}$. Obviously, matrix \mathbf{A} depends on the solution $\Delta \mathbf{x}$ to the minimization problem (3), implying that the constraints in (3) are nonlinear. Usually, an iteration method is used.

Before deciding which level to change, the values of $\partial T/\partial z$ and $\partial S/\partial z$, the gradients of temperature and salinity between two adjacent levels involved in the instability, are examined. This helps determine if the temperature or salinity profile, or both, are to be changed to stabilize the density field. If $\partial T/\partial z < 0$, $\partial S/\partial z < 0$, only temperature is changed; if $\partial T/\partial z > 0$, $\partial S/\partial z > 0$, only salinity is changed; and if $\partial T/\partial z < 0$, $\partial S/\partial z > 0$, both temperature and salinity fields are adjusted with a local linear trend test (Locarnini et al. 2006). Here, the z axis points upward. The principle is to stabilize the hydrographic profiles with minimum adjustment.

The benefit of using the MA method can be easily identified from comparison between two ocean atlases: the ocean atlas of Levitus (1982; without MA) and the *World Ocean Atlas 2005* (Locarnini et al. 2006; with MA). Both atlases consist of annually and monthly averaged vertical profiles of temperature and salinity on a global $1^\circ \times 1^\circ$ grid at 33 vertical levels. The ocean atlas of Levitus (1982) has considerable casts possessing static instability; however, the *World Ocean Atlas 2005* contains no profile possessing static instability.

To eliminate the static instability, the MA method does not require the conservation of heat and salt. Because one of the ocean's important roles in the earth's climate is heat transport, an adjustment made without taking heat conservation into account may lead to errors in estimating the ocean's impact on global climate change. In this study, a new conserved scheme is developed to simultaneously adjust the temperature and salinity profiles from (T_k, S_k) to $(T_k + \Delta T_k, S_k + \Delta S_k)$. A set of $2K$ algebraic (linear and nonlinear) equations are established to get $(\Delta T_k, \Delta S_k)$ on the base of heat and salt conservation, predetermined $(\Delta T_k/\Delta S_k)$ ratios (or called adjustment ratios) for all levels, and the removal of static instability by adjusting E_k to $E_k + \Delta E_k$ with a combined conservation and nonuniform increment treatment.

2. Unconserved adjustment

An example as described in appendix B of Locarnini et al. (2006) is used for illustration. The area chosen for

this example is the 1° latitude–longitude box centered at 53.5°S , 171.5°E from Levitus et al. (1998). This is on the New Zealand Plateau, with a bottom depth below 1000 m and above 1100 m. The month is October, during the early austral summer. There is no temperature or salinity data within the chosen 1° box. Thus, the objectively analyzed values in this 1° box will be dependent on the seasonal objectively analyzed field and the data in nearby 1° grid boxes. There is much more temperature data than salinity data on the New Zealand Plateau for October. This contributes to six small (on the order of $10^{-2} \text{ kg m}^{-3}$) inversions in the local potential density field calculated from objectively analyzed temperature and salinity fields (Table 1). After using the MA method, the original and adjusted profiles $\{T_k, S_k, k = 1, 2, \dots, K\}$ are as shown in Fig. 1, and the adjusted temperature and salinity profiles are listed in Table 2. Readers are referred to appendix B of Locarnini et al. (2006) for detailed information on the stabilization procedures. The relative root-mean adjustment (RRMA) using the MA method can be represented by

$$\begin{aligned} \text{RRMA} &= \frac{\sqrt{\frac{1}{K} \sum_{k=1}^K (\Delta T_k)^2}}{\max(T_k) - \min(T_k)} + \frac{\sqrt{\frac{1}{K} \sum_{k=1}^K (\Delta S_k)^2}}{\max(S_k) - \min(S_k)} \\ &= 0.0712. \end{aligned} \quad (4)$$

RRMA represents the mean adjustment relative to the range of a profile. The total heat and salt changes of the water column within this $1^\circ \times 1^\circ$ grid box are estimated by

$$\Delta Q = A \rho_0 c_p \int_{-H}^0 \Delta T dz, \quad \Delta(\text{salt}) = A \int_{-H}^0 \Delta S dz,$$

where ρ_0 ($=1028 \text{ kg m}^{-3}$) is the characteristic density, c_p ($=4002 \text{ J kg}^{-1} \text{ K}^{-1}$) is the specific heat for the seawater, $H = 1000 \text{ m}$, and A is the area of the grid box,

$$A = \left(\frac{\pi}{180} R\right)^2 \cos \varphi,$$

where R ($=6370 \text{ km}$) is the earth's radius, and φ ($=53.5^\circ$) is the latitude of the grid box. The temperature and salinity adjustments $(\Delta T, \Delta S)$ are obtained by comparison between Tables 1 and 2, the heat and salt changes of the water column for this grid box are calculated by

$$\Delta Q = -7.0411 \times 10^{17} \text{ J}, \quad \Delta(\text{salt}) = -0.5443 \times 10^{10} \text{ kg}.$$

Because one of the ocean's important roles in the earth's climate is transporting heat from low to high latitudes, nontrivial heat and salt losses show that the unconserved

TABLE 1. Grid box 171.5°E, 53.5°S Levitus et al. (1998) profiles before stabilization (from Locarnini et al. 2006, Table B1). Here, the asterisks in the last column indicate the static instability.

k	Depth (m)	T (°C)	S (ppt)	$\rho(S_{k+1}, T_{k+1}, z_k)$ (kg m ⁻³)	$\rho(S_k, T_k, z_k)$ (kg m ⁻³)	E_k (kg m ⁻³)
1	0	7.1667	34.4243	26.9476	26.9423	0.0054
2	10	7.1489	34.4278	26.8982	26.9939	-0.0957*
3	20	7.0465	34.2880	26.9529	26.9443	0.0085
4	30	7.0050	34.2914	27.0104	26.9990	0.0114
5	50	6.9686	34.2991	27.0967	27.1028	-0.0061*
6	75	7.0604	34.3073	27.2406	27.2120	0.0286
7	100	6.9753	34.3280	27.3892	27.3560	0.0332
8	125	6.9218	34.3604	27.5164	27.5046	0.0117
9	150	6.8919	34.3697	27.6000	27.6316	-0.0316*
10	200	6.9363	34.3364	27.8123	27.8302	-0.0179*
11	250	7.0962	34.3415	28.0295	28.0421	-0.0126*
12	300	7.1622	34.3367	28.2684	28.2593	0.0092
13	400	6.8275	34.2852	28.6664	28.7281	-0.0618*
14	500	7.4001	34.3123	29.3699	29.1238	0.2461
15	600	6.2133	34.4022	29.9386	29.8292	0.1094
16	700	5.9186	34.4868	30.5869	30.3978	0.1891
17	800	4.5426	34.4904	31.0754	31.0488	0.0266
18	900	4.1263	34.4558	31.6539	31.5377	0.1162
19	1000	3.3112	34.4755		32.1176	

adjustment may change heat transport and in turn affect the overturning thermohaline circulation.

$$E_{k_i}^* = E_{\min}, \tag{5}$$

3. Stabilization

The stabilization process is divided into three parts: 1) stability increasing at unstable levels, 2) stability decreasing at stable levels, and 3) normalization for conservation of stability for the cast. Let static instability occur at level k_1, k_2, \dots, k_i [i.e., satisfies the inequality (2)], the static stability E_{k_i} is increased to its marginal stability value ($E_{k_i}^*$),

that is, the *minimal adjustment* with increment of

$$\Delta E_{k_i} = E_{\min} - E_{k_i}.$$

Such an increase of stability will be compensated by the decrease of stability at neighboring levels $k_i \pm m$ ($m = 1, 2, \dots$) with skipping the unstable levels until reaching the top and bottom of the profile,

$$E_{k_i \pm m}^* = \begin{cases} E_{k_i \pm m} - \Delta E_{k_i} / 2^{m+1} & \text{if } E_{k_i \pm m} - \Delta E_{k_i} / 2^{m+1} \geq E_{\min} \\ E_{\min} & \text{if } E_{k_i \pm m} - \Delta E_{k_i} / 2^{m+1} < E_{\min} \end{cases}.$$

The static stabilities for the whole profile before and after the adjustment are calculated by

$$I = \sum_{k=1}^K E_k, \quad I^* = \sum_{k=1}^K E_k^*. \tag{6}$$

The normalization process is conducted by

$$E_k^{**} = \frac{I}{I^*} E_k^* \tag{7}$$

to keep the *conservation of the static stability* for each profile. After three stabilization processes, the static stability is represented by [see Eq. (1)]

$$\rho(S_{k+1} + \Delta S_{k+1}, T_{k+1} + \Delta T_{k+1}, z_k) - \rho(S_k + \Delta S_k, T_k + \Delta T_k, z_k) = E_k^{**}, \quad k = 1, 2, \dots, K - 1. \tag{8}$$

When E_{\min} is specified [see Eq. (5)], the right-hand side of (8) (i.e., E_k^{**}) is the known adjustment, which is calculated through (5)–(7). Equation (8) is used to determine the temperature and salinity adjustments at each depth for given E_k^{**} . The difference between (7) (i.e., the direct determination of E_k^{**}) and (8) is that (7) shows the minimal density adjustment to remove static instability, and (8) is to calculate the (T, S) adjustment at each depth.

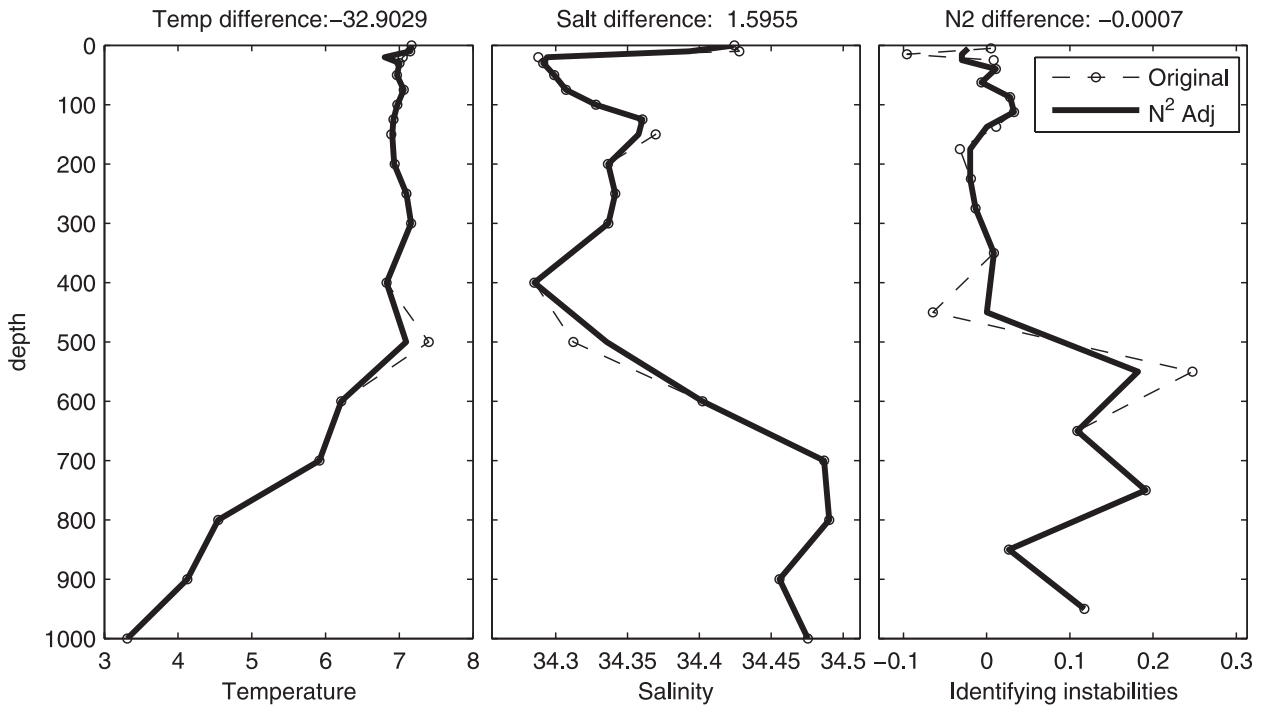


FIG. 1. Original (dashed) and adjusted (solid) profiles temperature of T_k , salinity S_k , and static stability E_k at the grid box 53.5°S, 171.5°E using the MA method (Locarnini et al. 2006).

4. Constraints for temperature and salinity adjustment

$$\int_{-h}^0 \Delta T dz = 0, \quad \int_{-h}^0 \Delta S dz = 0, \quad (9)$$

Conservation of heat and salt for the adjustment can be represented by

which can be discretized by

TABLE 2. Grid box 53.5°S, 171.5°E improved Levitus et al. (1998) profiles after stabilization using the MA method (from Locarnini et al. 2006, Table B2).

k	Depth (m)	T (°C)	S (ppt)	$\rho(S_{k+1}, T_{k+1}, z_k)$ (kg m^{-3})	$\rho(S_k, T_k, z_k)$ (kg m^{-3})	E_k (kg m^{-3})
1	0	7.1667	34.3096	26.8521	26.8519	0.0002
2	10	7.1489	34.3063	26.8982	26.8982	0.0000
3	20	7.0465	34.2880	26.9529	26.9443	0.0085
4	30	7.0050	34.2914	27.0042	26.9990	0.0051
5	50	7.0132	34.2991	27.0967	27.0967	0.0000
6	75	7.0604	34.3073	27.2361	27.2120	0.0240
7	100	6.9796	34.3228	27.3513	27.3513	0.0000
8	125	6.9897	34.3243	27.4667	27.4667	0.0000
9	150	7.0242	34.3301	27.5820	27.5820	0.0000
10	200	7.0628	34.3364	27.8123	27.8123	0.0000
11	250	7.0962	34.3415	28.0422	28.0421	0.0000
12	300	7.0748	34.3367	28.2719	28.2719	0.0001
13	400	6.8275	34.2894	28.7314	28.7314	0.0000
14	500	6.9604	34.3123	29.3699	29.1899	0.1799
15	600	6.2133	34.4022	29.9386	29.8292	0.1094
16	700	5.9186	34.4868	30.5869	30.3978	0.1891
17	800	4.5426	34.4904	31.0754	31.0488	0.0266
18	900	4.1263	34.4558	31.6539	31.5377	0.1162
19	1000	3.3112	34.4755		32.1176	

TABLE 3. Change of $(T_k + \Delta T_k^{(j)})$ ($^{\circ}\text{C}$) at each iteration using the Newton's method. It is noted that the iteration converges at the third iteration.

k	Depth (m)	$j = 0$	$j = 1$	$j = 2$	$j = 3$	$j = 4$
1	0	7.166 700	7.212 634	7.212 833	7.212 833	7.212 833
2	10	7.148 900	7.289 401	7.289 072	7.289 072	7.289 072
3	20	7.046 500	6.818 173	6.816 828	6.816 828	6.816 828
4	30	7.005 000	6.872 865	6.872 591	6.872 591	6.872 591
5	50	6.968 600	6.888 794	6.888 861	6.888 861	6.888 861
6	75	7.060 400	7.023 494	7.023 712	7.023 712	7.023 712
7	100	6.975 300	6.977 379	6.977 638	6.977 638	6.977 638
8	125	6.921 800	6.965 175	6.965 378	6.965 378	6.965 378
9	150	6.891 900	6.983 992	6.983 997	6.983 997	6.983 997
10	200	6.936 300	6.959 537	6.959 779	6.959 779	6.959 779
11	250	7.096 200	7.125 999	7.126 229	7.126 229	7.126 229
12	300	7.162 200	7.228 075	7.228 205	7.228 205	7.228 205
13	400	6.827 500	6.995 044	6.994 489	6.994 488	6.994 488
14	500	7.400 100	7.229 221	7.228 652	7.228 652	7.228 652
15	600	6.213 300	6.129 374	6.129 400	6.129 400	6.129 400
16	700	5.918 600	5.883 923	5.884 121	5.884 121	5.884 121
17	800	4.542 600	4.542 873	4.543 127	4.543 127	4.543 127
18	900	4.126 300	4.153 784	4.154 020	4.154 020	4.154 020
19	1000	3.311 200	3.362 894	3.363075	3.363 075	3.363 075

$$\sum_{k=1}^{K-1} \frac{(\Delta T_k + \Delta T_{k+1})}{2} (z_k - z_{k+1}) = 0, \quad (10)$$

$$\sum_{k=1}^{K-1} \frac{(\Delta S_k + \Delta S_{k+1})}{2} (z_k - z_{k+1}) = 0. \quad (11)$$

Equations (10) and (11) can be rewritten by

$$\sum_{k=1}^K a_k \Delta T_k = 0, \quad \sum_{k=1}^K a_k \Delta S_k = 0, \quad (12)$$

where

$$a_1 = \frac{z_1 - z_2}{2(z_1 - z_K)}, \quad a_2 = \frac{z_1 - z_3}{2(z_1 - z_K)}, \quad a_3 = \frac{z_2 - z_4}{2(z_1 - z_K)}, \quad \dots, \quad a_{K-1} = \frac{z_{K-2} - z_K}{2(z_1 - z_K)}, \quad a_K = \frac{z_{K-1} - z_K}{2(z_1 - z_K)}. \quad (13)$$

Obviously, we have

$$\sum_{k=1}^K a_k = 1, \quad a_k > 0 \quad \text{for } k = 1, 2, \dots, K. \quad (14)$$

The adjustment ratios γ_k are used for $N - 1$ levels,

$$\Delta T_k + \gamma_k \Delta S_k = 0, \quad k = 1, 2, \dots, K - 1. \quad (15)$$

Because temperature and salinity corrections affect the density differently, that is, the increase (decrease) of temperature (salinity) decreases (increases) the density. This leads to a positive value of γ_k . Here, we use the simplest form,

$$\gamma_k = \gamma \equiv \frac{\max(T_k) - \min(T_k)}{\max(S_k) - \min(S_k)}, \quad (16)$$

to illustrate the basic methodology of this analytical adjustment procedure. This ratio may vary with depth. A large part of the paper by Jackett and McDougall (1995) was devoted to developing a method to determine γ_k . Interested readers are referred to their paper.

Equations (10), (11), (15), and (8) represent a set of $2K$ algebraic equations for $2K$ unknowns $(\Delta T_k, \Delta S_k)$, $k = 1, 2, \dots, K$. Thus, they are closure. Among them, (8) is nonlinear and (10), (11), and (15) are linear.

5. Example

The same example as described in section 2 is used. Substitution of $\{S_k, T_k, z_k\}$ values from Table 1 into (8), (10), (11), and (15), and the Newton iteration method (Kelley 1987, see appendix B) is used to solve the set of $2K$ algebraic equations. For the hydrographic cast listed in Table 1, only three iterations are needed to eliminate the static instability. Tables 3 and 4 list the values of

TABLE 4. Change of $(S_k + \Delta S_k^{(j)})$ (ppt) at each iteration using Newton's method. It is noted that the iteration converges at the third iteration.

k	Depth (m)	$j = 0$	$j = 1$	$j = 2$	$j = 3$	$j = 4$
1	0	34.424 300	34.421 995	34.421 985	34.421 985	34.421 985
2	10	34.427 800	34.420 749	34.420 765	34.420 765	34.420 765
3	20	34.288 000	34.299 459	34.299 526	34.299 526	34.299 526
4	30	34.291 400	34.298 031	34.298 045	34.298 045	34.298 045
5	50	34.299 100	34.303 105	34.303 102	34.303 102	34.303 102
6	75	34.307 300	34.309 152	34.309 141	34.309 141	34.309 141
7	100	34.328 000	34.327 896	34.327 883	34.327 883	34.327 883
8	125	34.360 400	34.358 223	34.358 213	34.358 213	34.358 213
9	150	34.369 600	34.364 978	34.364 978	34.364 978	34.364 978
10	200	34.336 400	34.335 234	34.335 222	34.335 222	34.335 222
11	250	34.341 500	34.340 005	34.339 993	34.339 993	34.339 993
12	300	34.336 700	34.333 394	34.333 388	34.333 388	34.333 388
13	400	34.285 200	34.276 792	34.276 820	34.276 820	34.276 820
14	500	34.312 300	34.320 875	34.320 904	34.320 904	34.320 904
15	600	34.402 200	34.406 412	34.406 410	34.406 410	34.406 410
16	700	34.486 800	34.488 540	34.488 530	34.488 530	34.488 530
17	800	34.490 400	34.490 386	34.490 374	34.490 374	34.490 374
18	900	34.455 800	34.454 421	34.454 409	34.454 409	34.454 409
19	1000	34.475 500	34.472 906	34.472 897	34.472 897	34.472 897

$\{T_k, S_k\}$ at the each iteration. They show the high efficiency of this method for elimination of static instability in the hydrographic cast. Figure 2 shows the original and adjusted profiles

$$\{S_k, T_k, E_k\}, \quad k = 1, 2, \dots, K. \quad (17)$$

The heat and salt are conserved for the whole water column with the relative root-mean adjustment

$$RRMA = 0.0482. \quad (18)$$

Comparing (18) to (4), we may find that this analytical conserved adjustment scheme has a smaller RRMA (0.0482) than the MA method (0.0712).

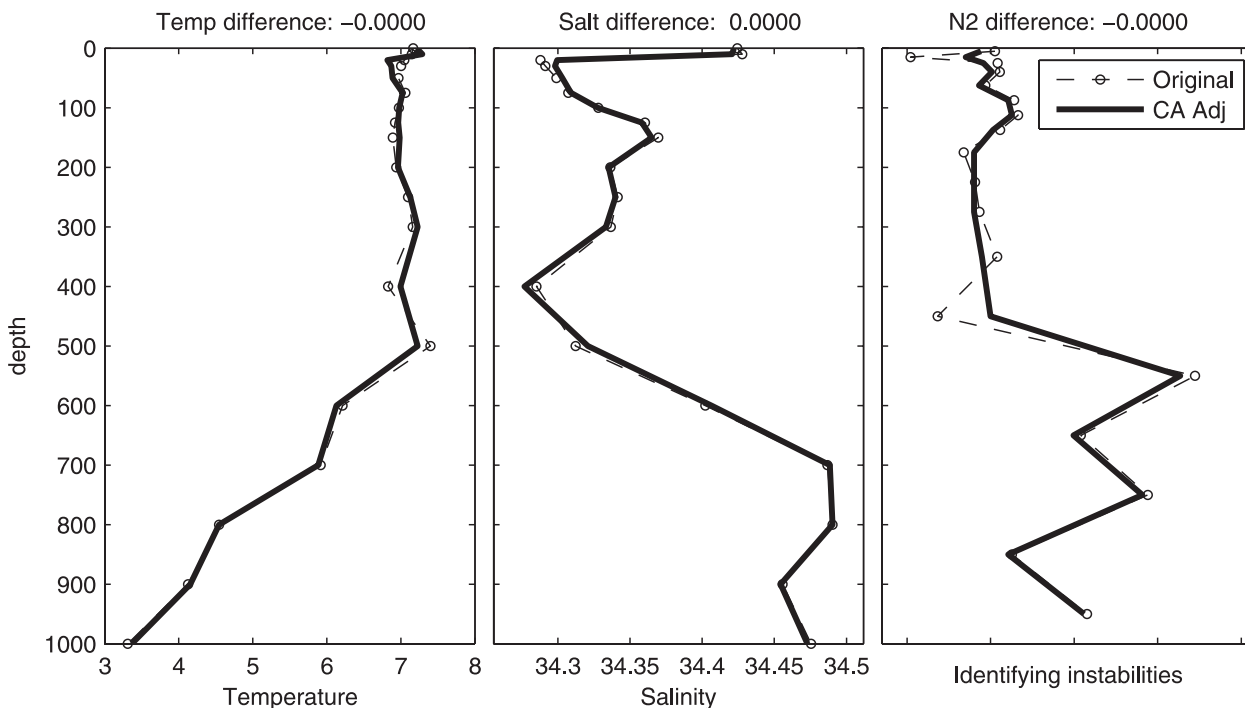


FIG. 2. As in Fig. 1, but using the analytical conserved method proposed in this paper.

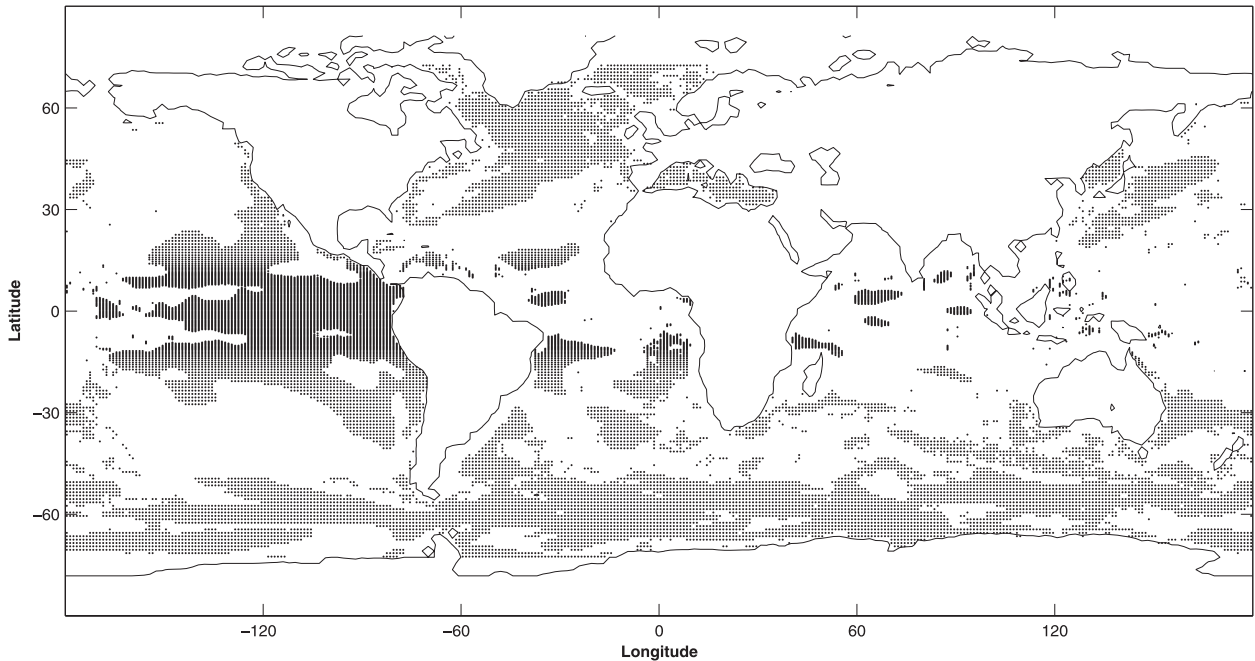


FIG. 3. Distribution of statically unstable casts in the JPL-ECCO 10-day data centered on 31 Dec 2008 (available online at <http://ecco.jpl.nasa.gov/external/>). The data were produced by a data assimilation system.

Data assimilation is required in operational ocean data access and retrieval (Sun 1999). It is to blend the modeled variable \mathbf{x}_m with observational data \mathbf{y}_o (e.g., Kalnay 2003; Chu et al. 2004),

$$\mathbf{x}_a = \mathbf{x}_m + \mathbf{W} \cdot [\mathbf{y}_o - H(\mathbf{x}_m)], \quad (19)$$

where \mathbf{x}_a is the assimilated variable, H is an operator that provides the model's theoretical estimate of what is observed at the observational points, and \mathbf{W} is the weight matrix. The difference among various data assimilation schemes such as optimal interpolation (e.g., Lozano et al. 1996), Kalman filter (e.g., Galanis et al. 2006), and variation methods (e.g., Tang and Kleeman 2004), is the different ways to determine the weight matrix \mathbf{W} . The data assimilation process (19) can be considered as the average (in a generalized sense) of \mathbf{x}_m and \mathbf{y}_o . In ocean (T, S) data assimilation, the observational data \mathbf{y}_o may contain several casts, which are statically stable. The model profile \mathbf{x}_m is also statically stable because convective adjustment (Bryan 1969) is usually conducted at each time step.

False static stability may be generated after (T, S) data assimilation [i.e., performing (19)]. For example, 10-day Jet Propulsion Laboratory (JPL) Estimating the Circulation and Climate of the Ocean (ECCO) (T, S) fields centered on 31 December 2008 (available online at <http://ecco.jpl.nasa.gov/external/>) show that a considerable portion (35.32%) of profiles are statically unstable

(Fig. 3). Here, the NODC's criterion for flagging out statically unstable profiles,

$$E_{\min} = \begin{cases} -0.03 \text{ kg m}^{-3} & (0 \geq z_k \geq -30 \text{ m}) \\ -0.02 \text{ kg m}^{-3} & (-30 \text{ m} > z_k \geq -400 \text{ m}), \\ 0 \text{ kg m}^{-3} & (-400 \text{ m} > z_k) \end{cases}, \quad (20)$$

is used. Because such a false static instability is due to the blending of observational data with the model data, it is not a real instability. Use of the convective adjustment scheme may overcorrect the profiles.

To illustrate this, we discuss the existing convective adjustment schemes in ocean models. The various convective adjustment schemes are based on the same original idea (e.g., Bryan 1969): whenever a water column is statically unstable, temperature and salinity are vertically adjusted to make the water column neutrally stable, with heat and salt conserved in the process. The adjustment takes an iterative approach. The iteration continues between all adjacent levels until the static instability is removed in the whole water column. Because the adjustment acts on only neighboring points, the number of iterations required to reach the final stable state is infinite for a given unstable profile (Smith 1989). In practice, however, the number of iteration is always finite, and this leads to some residual instability (Killworth 1989).

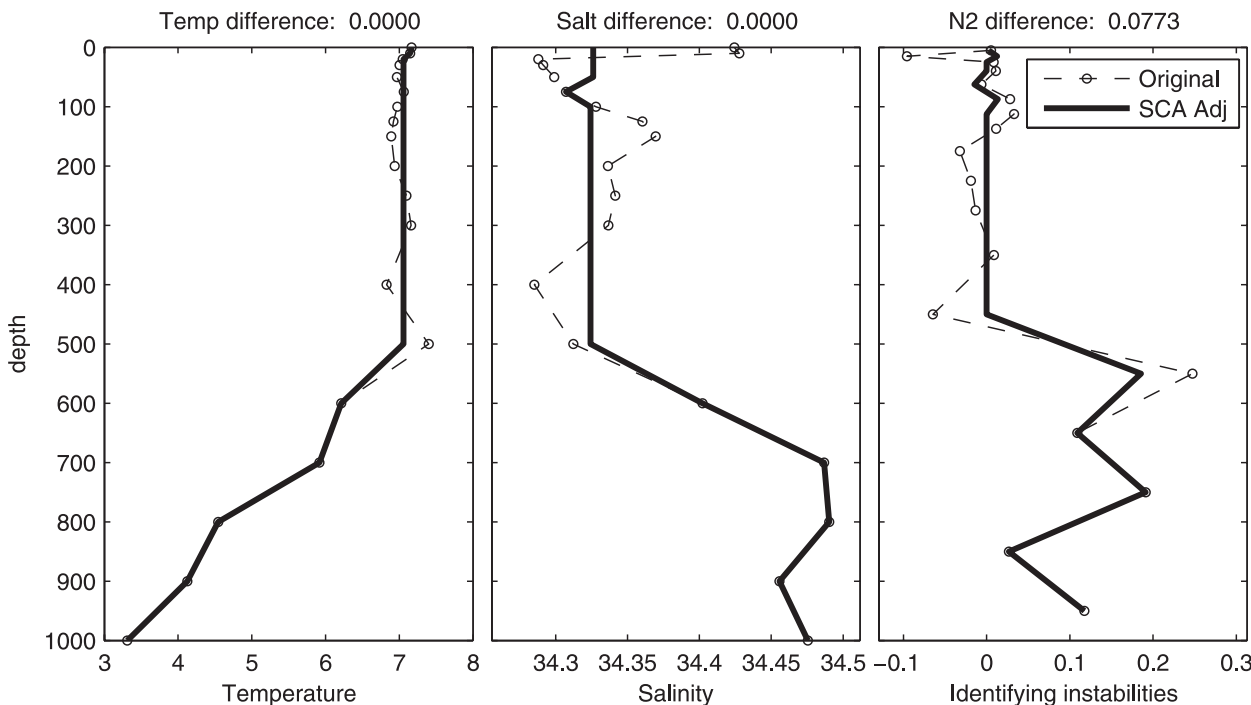


FIG. 4. As in Fig. 1, but using the complete convective adjustment method (Yin and Sarachik 1994).

Several algorithms were developed to remove these residual static instabilities such as the implicit vertical diffusion scheme (Cox 1984; Killworth 1989) and the complete adjustment scheme (Yin and Sarachik 1994). The former tests the static stability between the vertically adjacent levels and, if unstable, the vertical diffusivity is set to a large value (convective diffusivity) to smooth out the instability. The latter determines the upper and lower boundaries of each adjusted region while keeping the instantaneous adjustment within each unstable region. Yin and Sarachik (1994) showed that the complete convective adjustment scheme is more efficient than the implicit vertical diffusion scheme and guaranteed a complete removal of static instability of a water column at each time step. For the same example as described in section 2, the complete convective adjustment scheme removes the static instabilities (Fig. 4) with the relative root-mean adjustment

$$RRMA = 0.2192. \tag{21}$$

This value is 4.5 times larger than that of (0.0482) using the analytical adjustment method.

6. Conclusions

A new analytical conserved adjustment scheme is developed to eliminate the static instability of raw and averaged observational hydrographic data. This method

adjusts the temperature and salinity profiles $\{\Delta T_k, \Delta S_k, k = 1, 2, \dots, K\}$ simultaneously and efficiently on the basis of three types of constraints: 1) heat and salt conservation, 2) predetermined $(\Delta T_k/\Delta S_k)$ ratios (or called adjustment ratios) for all levels, and 3) the removal of static instability by adjusting the static stability with a combined conservation and nonuniform increment treatment. With these constraints, a set of $2K$ combined linear/nonlinear algebraic equations are established for $\{\Delta T_k, \Delta S_k\}$. Among them, $(K + 1)$ algebraic equations are linear, and $(K - 1)$ equations are nonlinear. Newton's method is used to solve this set of equations. The proposed scheme has very small relative root-mean-square adjustment compared to the existing methods. Moreover, it has three features: 1) conservation of heat and salt, 2) removal of static instabilities with small (T, S) adjustments, and 3) analytical form. With these features, it can be widely used in ocean (T, S) data analysis. Besides, ocean data assimilation may cause false static instabilities. Because this instability is not real, commonly used convective adjustment schemes may over-adjust the profiles. Therefore, the proposed analytical conserved scheme can be used in ocean (T, S) data assimilation.

Acknowledgments. The Office of Naval Research, the Naval Oceanographic Office, and the Naval Postgraduate School supported this study.

APPENDIX A

Validity of the Conservation Constraints

In ocean modeling, all the convective adjustment schemes for stabilizing (T, S) profiles require heat and salt conservation (e.g., Yin and Sarachik 1994). In ocean data analysis, such conservation constraints are also valid. After quality control procedures, it is reasonable to assume that ocean observational data ψ contain random error ψ' ,

$$\psi = \psi' + \psi', \quad (\text{A1})$$

with population mean $\langle \psi' \rangle = 0$ and standard deviation σ_e . Here, ψ denotes (T, S) , and ψ' is the true value at the same location and time as the observation taken place. The population mean of (A1) gives

$$\langle \psi \rangle = \langle \psi' \rangle. \quad (\text{A2})$$

An observational profile $(\psi_k, k = 1, 2, \dots, K)$ can be taken as a sample. Vertical integration of the observational profile is represented by weighted average [see (12)],

$$\langle \bar{\psi} \rangle = \sum_{k=1}^K a_k \psi_k, \quad \langle \bar{\psi}' \rangle = \sum_{k=1}^K a_k \psi'_k, \quad \langle \bar{\psi}' \rangle = \sum_{k=1}^K a_k \psi'_k. \quad (\text{A3})$$

The random errors at different depth ψ'_k are considered independent. The central limit theorem states that the linear combination

$$Y' = \sum_{k=1}^K a_k \psi'_k \quad (\text{A4})$$

has a normal distribution with zero mean and variance,

$$\sigma_{Y'}^2 = \sum_{k=1}^K a_k^2 \sigma_e^2 = \sigma_e^2 \sum_{k=1}^K a_k^2. \quad (\text{A5})$$

From (14), we have

$$\sum_{k=1}^K a_k^2 < \sum_{k=1}^K a_k = 1. \quad (\text{A6})$$

Substitution of (A6) into (A5) leads to

$$\sigma_{Y'} < \sigma_e, \quad (\text{A7})$$

which indicates that the error variance of the vertically integrated observed values $\bar{\psi}$ is smaller than that of the

individual observations σ_e . Thus, the conservation constraints (10) and (11) guarantee that

$$\langle \bar{\psi}^{\text{adj}} \rangle = \langle \bar{\psi}' \rangle + \langle \bar{\psi}' \rangle, \quad (\text{A8})$$

the same smaller error variance of the vertically integrated observed values.

APPENDIX B

Newton Method

Let the temperature and salinity adjustment be represented by a $2K$ -dimensional vector \mathbf{P} ,

$$\mathbf{P} \equiv \begin{bmatrix} p_1 \\ p_2 \\ p_3 \\ p_4 \\ \vdots \\ \vdots \\ \vdots \\ p_{M-1} \\ p_M \end{bmatrix} = \begin{bmatrix} \Delta T_1 \\ \Delta S_1 \\ \Delta T_2 \\ \Delta S_2 \\ \vdots \\ \vdots \\ \vdots \\ \Delta T_K \\ \Delta S_K \end{bmatrix}, \quad M = 2K. \quad (\text{B1})$$

The algebraic Eqs. (10), (11), (15), and (8) [note that we put (8) at the last] can be represented by

$$\mathbf{F}(\mathbf{P}) = 0, \quad (\text{B2})$$

where \mathbf{F} has the dimension of $2K$. The classical Newton method (Kelley 1987) for approximating a desired solution \mathbf{P} to (B2) is formally defined by the iteration

$$\mathbf{P}^{(j+1)} = \mathbf{P}^{(j)} - \mathbf{J}^{-1}(\mathbf{P}^{(j)})\mathbf{F}(\mathbf{P}^{(j)}), \quad j = 0, 1, 2, \dots, \quad (\text{B3})$$

where $\mathbf{P}^{(j)}$ is the j th approximation to the solution of (B2), $\mathbf{J}(\mathbf{P}^{(j)})$ is the Jacobian matrix of $\mathbf{F}(\mathbf{P})$ evaluated at $\mathbf{P}^{(j)}$. Inversion of the Jacobian matrix is not performed in practice; rather (B3) is implemented via solution of the following system of linear equations at the each iteration:

$$\mathbf{J}(\mathbf{P}^{(j)}) \cdot \mathbf{d}^{(j)} = \mathbf{b}^{(j)}, \quad \mathbf{b}^{(j)} \equiv -\mathbf{F}(\mathbf{P}^{(j)}), \quad (\text{B4})$$

followed by the update

$$\mathbf{P}^{(j+1)} = \mathbf{P}^{(j)} + \mathbf{d}^{(j)}, \quad (\text{B5})$$

where $\mathbf{d}^{(j)}$ is called the Newton direction. The iteration stops at step J when

$$\max_k |d_k^{(j)}| < 10^{-6} \text{ (K for temperature and ppt for salinity).} \tag{B6}$$

When the set of algebraic equations take the order of (10), (11), (15), and (8), the Jacobian matrix $\mathbf{J}(\mathbf{P}^{(j)})$ with dimension of $M \times M$ is represented by

$$\mathbf{J}(\mathbf{P}^{(j)}) = \begin{bmatrix} a_{11} & a_{12} & \dots & a_{1M} \\ a_{21} & a_{22} & \dots & a_{2M} \\ \dots & \dots & \dots & \dots \\ a_{M1} & a_{M2} & \dots & a_{MM} \end{bmatrix}, \tag{B7}$$

where the $M \times M$ elements are given in (C1) of appendix C. The Jacobian matrix (B7) has the following format with many zero elements:

$$\mathbf{J}(\mathbf{P}^{(j)}) = \begin{bmatrix} * & 0 & * & 0 & * & 0 & \dots & \dots & * & 0 \\ 0 & * & 0 & * & 0 & * & \dots & \dots & 0 & * \\ * & * & 0 & 0 & 0 & 0 & \dots & \dots & 0 & 0 \\ * & * & * & * & 0 & 0 & \dots & \dots & 0 & 0 \\ 0 & 0 & * & * & 0 & 0 & \dots & \dots & 0 & 0 \\ 0 & 0 & * & * & * & * & \dots & \dots & 0 & 0 \\ \dots & \dots & \dots & \dots & \dots & \dots & \dots & \dots & \dots & \dots \\ \dots & \dots & \dots & \dots & \dots & \dots & \dots & \dots & \dots & \dots \\ 0 & 0 & 0 & 0 & \dots & \dots & * & * & 0 & 0 \\ 0 & 0 & 0 & 0 & \dots & \dots & * & * & * & * \end{bmatrix}, \tag{B8}$$

where nonzero elements are indicated by asterisks. The vector \mathbf{b} in the right-hand side of (B4) has the following components:

$$\begin{aligned} b_1 &= 0, & b_2 &= 0, & b_3 &= 0, & b_4 &= E_1^{**} - \rho(S_1 + \Delta S_1^{(j)}, T_1 + \Delta T_1^{(j)}, z_1) + \rho(S_2 + \Delta S_2^{(j)}, T_2 + \Delta T_2^{(j)}, z_2), \\ b_5 &= 0, & b_6 &= E_2^{**} - \rho(S_2 + \Delta S_2^{(j)}, T_2 + \Delta T_2^{(j)}, z_2) + \rho(S_3 + \Delta S_3^{(j)}, T_3 + \Delta T_3^{(j)}, z_2), \dots, & b_{M-1} &= 0, \\ b_M &= E_{K-1}^{**} - \rho(S_{K-1} + \Delta S_{K-1}^{(j)}, T_K + \Delta T_{K-1}^{(j)}, z_{K-1}) + \rho(S_K + \Delta S_K^{(j)}, T_K + \Delta T_K^{(j)}, z_{K-1}). \end{aligned} \tag{B9}$$

It is noted that the well-posed linear algebraic Eq. (A4) is easily solved with the initial guess,

$$\mathbf{P}^{(0)} = 0, \tag{B10}$$

that is,

$$\Delta T_k^{(0)} = 0, \quad \Delta S_k^{(0)} = 0, \quad k = 1, 2, \dots, K. \tag{B11}$$

With the initial guess (B11), the Newton direction $\mathbf{d}^{(0)}$ is obtained from solving the linear algebraic Eq. (B4). The vector $\mathbf{d}^{(0)}$ is added to the initial guess $\mathbf{P}^{(0)}$, which leads to

$$\mathbf{P}^{(1)} = \mathbf{P}^{(0)} + \mathbf{d}^{(0)}. \tag{B12}$$

With $\mathbf{P}^{(1)}$, the cast is adjusted to its first iterated values,

$$S_k^{(1)} = S_k + \Delta S_k^{(1)}, \quad T_k^{(1)} = T_k + \Delta T_k^{(1)}. \tag{B13}$$

Substitution of (B12) into (1) gives static stability after the first iteration $E_k^{(1)}$. If

$$E_k^{(1)} \geq E_{\min}, \quad k = 1, 2, \dots, K, \tag{B14}$$

the adjustment stops. Otherwise, the iteration continues, that is, the linear algebraic Eq. (B4) is solved after using $\mathbf{P}^{(1)}$ from (B12). Addition of the solution $\mathbf{d}^{(1)}$ to $\mathbf{P}^{(1)}$ leads to $\mathbf{P}^{(2)}$. If there is no static instability, the adjustment stops. Otherwise, the iteration continues until the static instability is eliminated.

APPENDIX C

Elements of Jacobian Matrix (B7)

The elements of $M \times M$ Jacobian matrix (B7) are given by

$$\begin{aligned} a_{11} &= \frac{\Delta z_1}{2}, & a_{13} &= \frac{\Delta z_1 + \Delta z_2}{2}, \dots, \\ a_{1,M-3} &= \frac{\Delta z_{N-2} + \Delta z_{N-1}}{2}, & a_{1,M-1} &= \frac{\Delta z_{N-1}}{2}, \\ a_{12} &= a_{14} = a_{16} = \dots = a_{1M} = 0, \\ a_{22} &= \frac{\Delta z_1}{2}, & a_{24} &= \frac{\Delta z_1 + \Delta z_2}{2}, \dots, \\ a_{2,M-2} &= \frac{\Delta z_{N-2} + \Delta z_{N-1}}{2}, & a_{2M} &= \frac{\Delta z_{N-1}}{2} \\ a_{21} &= a_{23} = a_{25} = \dots = a_{2,M-1} = 0, \\ a_{31} &= 1, & a_{32} &= \gamma_1, & a_{33} &= a_{34} = a_{35} = \dots = a_{3M} = 0, \end{aligned}$$

$$\begin{aligned}
a_{41} &= \frac{\partial \rho(S_1 + \Delta S_1^{(j)}, T_1 + T_1^{(j)}, z_2)}{\partial T} \\
&= -\rho(S_1 + \Delta S_1^{(j)}, T_1 + \Delta T_1^{(j)}, z_2) \alpha(S_1 + \Delta S_1^{(j)}, \\
&\quad T_1 + \Delta T_1^{(j)}, z_2), \\
a_{42} &= \frac{\partial \rho(S_1 + \Delta S_1^{(j)}, T_1 + \Delta T_1^{(j)}, z_2)}{\partial S} \\
&= \rho(S_1 + \Delta S_1^{(j)}, T_1 + \Delta T_1^{(j)}, z_2) \beta(S_1 + \Delta S_1^{(j)}, \\
&\quad T_1 + \Delta T_1^{(j)}, z_2), \\
a_{43} &= -\frac{\partial \rho(S_2 + \Delta S_2^{(j)}, T_2 + \Delta T_2^{(j)}, z_2)}{\partial T} \\
&= \rho(S_2 + \Delta S_2^{(j)}, T_2 + \Delta T_2^{(j)}, z_2) \alpha(S_2 + \Delta S_2^{(j)}, \\
&\quad T_2 + \Delta T_2^{(j)}, z_2), \\
a_{44} &= -\frac{\partial \rho(S_2 + \Delta S_2^{(j)}, T_2 + \Delta T_2^{(j)}, z_2)}{\partial S} \\
&= -\rho(S_2 + \Delta S_2^{(j)}, T_2 + \Delta T_2^{(j)}, z_2) \beta(S_2 + \Delta S_2^{(j)}, \\
&\quad T_2 + \Delta T_2^{(j)}, z_2), \\
a_{45} &= a_{46} = \dots = a_{4M} = 0, \\
a_{53} &= 1, \quad a_{54} = \gamma_2, \\
a_{51} &= a_{52} = a_{55} = a_{56} = a_{57} = \dots = a_{5M} = 0, \\
a_{63} &= \frac{\partial \rho(S_2 + \Delta S_2^{(j)}, T_2 + \Delta T_2^{(j)}, z_3)}{\partial T} \\
&= -\rho(S_2 + \Delta S_2^{(j)}, T_2 + \Delta T_2^{(j)}, z_3) \alpha(S_2 + \Delta S_2^{(j)}, \\
&\quad T_2 + \Delta T_2^{(j)}, z_3), \\
a_{64} &= \frac{\partial \rho(S_2 + \Delta S_2^{(j)}, T_2 + \Delta T_2^{(j)}, z_3)}{\partial S} \\
&= \rho(S_2 + \Delta S_2^{(j)}, T_2 + \Delta T_2^{(j)}, z_3) \beta(S_2 + \Delta S_2^{(j)}, \\
&\quad T_2 + \Delta T_2^{(j)}, z_3), \\
a_{65} &= -\frac{\partial \rho(S_3 + \Delta S_3^{(j)}, T_3 + \Delta T_3^{(j)}, z_3)}{\partial T} \\
&= \rho(S_3 + \Delta S_3^{(j)}, T_3 + \Delta T_3^{(j)}, z_3) \alpha(S_3 + \Delta S_3^{(j)}, \\
&\quad T_3 + \Delta T_3^{(j)}, z_3), \\
a_{66} &= -\frac{\partial \rho(S_3 + \Delta S_3^{(j)}, T_3 + \Delta T_3^{(j)}, z_3)}{\partial S} \\
&= -\rho(S_3 + \Delta S_3^{(j)}, T_3 + \Delta T_3^{(j)}, z_3) \beta(S_3 + \Delta S_3^{(j)}, \\
&\quad T_3 + \Delta T_3^{(j)}, z_3), \\
a_{61} &= a_{62} = a_{67} = a_{68} = \dots = a_{6M} = 0, \\
&\dots
\end{aligned}$$

$$\begin{aligned}
a_{M-1, M-3} &= 1, \quad a_{M-1, M-2} = \gamma_{N-1}, \\
a_{M-1, 1} &= a_{M-1, 2} = \dots = a_{M-1, M-4} \\
&= a_{M-1, M-1} = a_{M-1, M} = 0, \\
a_{M, M-3} &= \frac{\partial \rho(S_{K-1} + \Delta S_{K-1}^{(j)}, T_{K-1} + \Delta T_{K-1}^{(j)}, z_K)}{\partial T} \\
&= -\rho(S_{K-1} + \Delta S_{K-1}^{(j)}, T_{K-1} + \Delta T_{K-1}^{(j)}, z_K) \alpha(S_{K-1} \\
&\quad + \Delta S_{K-1}^{(j)}, T_{K-1} + \Delta T_{K-1}^{(j)}, z_K), \\
a_{M, M-2} &= \frac{\partial \rho(S_{K-1} + \Delta S_{K-1}^{(j)}, T_{K-1} + \Delta T_{K-1}^{(j)}, z_K)}{\partial S} \\
&= \rho(S_{K-1} + \Delta S_{K-1}^{(j)}, T_{K-1} + \Delta T_{K-1}^{(j)}, z_K) \beta(S_{K-1} \\
&\quad + \Delta S_{K-1}^{(j)}, T_{K-1} + \Delta T_{K-1}^{(j)}, z_K), \\
a_{M, M-1} &= -\frac{\partial \rho(S_K + \Delta S_K^{(j)}, T_K + \Delta T_K^{(j)}, z_K)}{\partial T} \\
&= \rho(S_K + \Delta S_K^{(j)}, T_K + \Delta T_K^{(j)}, z_K) \alpha(S_K + \Delta S_K^{(j)}, \\
&\quad T_K + \Delta T_K^{(j)}, z_K), \\
a_{MM} &= -\frac{\partial \rho(S_K + \Delta S_K^{(j)}, T_K + \Delta T_K^{(j)}, z_K)}{\partial S} \\
&= -\rho(S_K + \Delta S_K^{(j)}, T_K + \Delta T_K^{(j)}, z_K) \beta(S_K + \Delta S_K^{(j)}, \\
&\quad T_K + \Delta T_K^{(j)}, z_K), \quad \text{and} \\
a_{1M} &= a_{2, M} = \dots = a_{M-4, M} = 0. \tag{C1}
\end{aligned}$$

REFERENCES

- Bryan, K., 1969: A numerical method for the study of the circulation of the world ocean. *J. Comput. Phys.*, **4**, 347–376.
- Chu, P. C., G. H. Wang, and C. W. Fan, 2004: Evaluation of the U.S. Navy's Modular Ocean Data Assimilation System (MODAS) using the South China Sea Monsoon Experiment (SCSMEX) data. *J. Oceanogr.*, **60**, 1007–1021.
- Cox, M., 1984: A primitive equation, three-dimensional model of the ocean. GFDL Ocean Group Tech. Rep. 1, 143 pp.
- Galanis, G. N., P. Louka, P. Katsafados, G. Kallos, and I. Pytharoulis, 2006: Applications of Kalman filters based on nonlinear functions to numerical weather predictions. *Ann. Geophys.*, **24**, 2451–2460.
- Jackett, D. R., and T. J. McDougall, 1995: Minimal adjustment of hydrographic profiles to achieve static stability. *J. Atmos. Oceanic Technol.*, **12**, 381–389.
- Kalnay, E., 2003: *Atmospheric Modeling, Data Assimilation and Predictability*. Cambridge University Press, 341 pp.
- Kelley, C. T., 1987: *Solving Nonlinear Equations with Newton's Method (Fundamentals of Algorithms)*. SIAM, 103 pp.
- Killworth, P. D., 1989: On the parameterization of deep convection in ocean models. *Parameterization of Small Scale Processes: Proc. 'Aha Huliko'a Hawaiian Winter Workshop*, P. Muller, Ed., Hawaii Institute of Geophysics, 59–74.

- Levitus, S., 1982: *Climatological Atlas of the World Ocean*. NOAA Professional Paper 13, 173 pp.
- , 1998: *Introduction*. Vol. 1, *World Ocean Database 1998*, NOAA Atlas NESDIS 18, 346 pp.
- Locarnini, R. A., A. V. Mishonov, J. I. Antonov, T. P. Boyer, and H. E. Garcia, 2006: *Temperature*. Vol. 1, *World Ocean Atlas 2005*, NOAA Atlas NESDIS 61, 38 pp.
- Lozano, C. J., A. R. Robinson, H. G. Arrango, A. Gangopadhyay, Q. Sloan, P. J. Haley, L. Anderson, and W. Leslie, 1996: An interdisciplinary ocean prediction system: Assimilation strategies and structured data models. *Modern Approaches to Data Assimilation in Ocean Modeling*, P. Malanotte-Rizzoli, Ed., Elsevier, 413–452.
- Lynn, R. G., and J. L. Reid, 1968: Characteristics and circulation of deep and abyssal waters. *Deep-Sea Res.*, **15**, 577–598.
- Smith, N., 1989: The Southern Ocean thermohaline circulation: A numerical study. *J. Phys. Oceanogr.*, **19**, 713–726.
- Sun, L. C., 1999: Data inter-operability driven by oceanic data assimilation needs. *Mar. Technol. Soc. J.*, **33**, 55–66.
- Tang, Y., and R. Kleeman, 2004: SST assimilation experiments in a tropical Pacific Ocean model. *J. Phys. Oceanogr.*, **34**, 623–642.
- Yin, F. L., and E. S. Sarachik, 1994: An efficient convective adjustment scheme for ocean circulation models. *J. Phys. Oceanogr.*, **24**, 1425–1430.